The non-Hermitian skin effect: A perspective

Julius T. Gohsrich[1,2,a], Ayan Banerjee[1,b] and Flore K. Kunst[1,2,c]

[1] *Max Planck Institute for the Science of Light, Staudtstr. 2, 91058 Erlangen, Germany*
[2] *Department of Physics, Friedrich-Alexander Universität Erlangen-Nürnberg, Staudtstr. 7, 91058 Erlangen, Germany*
[a] julius.gohsrich@mpl.mpg.de   [b] ayan.banerjee@mpl.mpg.de   [c] flore.kunst@mpl.mpg.de

Abstract –The non-Hermitian (NH) skin effect is a truly NH feature, which manifests itself as an accumulation of states, known as skin states, on the boundaries of a system. In this perspective, we discuss several aspects of the NH skin effect focusing on the most interesting facets of this phenomenon. Non-normality and non-reciprocity are reviewed as necessary requirements to see the NH skin effect. We further discuss the NH skin effect as a topological effect that can be seen as a manifestation of a truly NH bulk-boundary correspondence, and show how topological boundary states can be distinguished from skin states. As most theoretical work has focused on studying the NH skin effect in the one-dimensional single-particle picture, recent developments of studying this effect in higher dimensions as well as in the many-body case are also highlighted. Lastly, experimental realizations and applications of the NH skin effect are reviewed.

Introduction. – Non-Hermitian (NH) topology has established itself as a new exciting research domain over the last decade [1–3]. Originally motivated from the fact that parity-time (PT) symmetric systems have a completely real eigenspectrum in the symmetry-unbroken regime [4, 5] and the subsequent surge in optical experiments [6–10], non-Hermiticity is increasingly studied in a wide variety of fields in physics ranging from mechanical [11], electrical [12], acoustic [13] and open quantum systems [14, 15] to strongly correlated phases of matter [16–23] and non-conservative biological systems [24, 25]. In the field of NH topology, non-Hermiticity is studied through the lens of condensed matter physics uncovering a remarkable enrichment of topological phenomena [1].

At the core of this enrichment is the fact that not only the eigenvectors but also the eigenvalues may have non-trivial topological features. Indeed, the spectrum now lives on the complex plane, such that eigenvalues may wind in a non-trivial manner captured by a spectral invariant [26–29] as illustrated in Fig. 1. It has been shown that topologically non-trivial spectral features in the eigenvalue spectrum under periodic boundary conditions (PBCs) result in macroscopic accumulation of states on the boundary of a lattice model under open boundary conditions (OBCs) [28–33] thus establishing a truly *non-Hermitian bulk-boundary correspondence* (BBC). These exponentially localized states are the so-called NH skin states, and the phenomenon over all is known as the *non-*

Hermitian skin effect, a term coined in Ref. 30, which is the central subject of this perspective.

Here we provide an overview of what we believe are the most interesting aspects of the NH skin effect. Besides a detailed discussion of the aforementioned NH BBC, we discuss how non-normality and non-reciprocity of NH matrices are necessary ingredients to observe the NH skin effect [34]. We continue by explicitly showing how the *biorthogonal properties* [35] of skin states allow us to distinguish them from topological boundary states. As the NH skin effect has predominantly been studied in the one-dimensional, single-particle case, we also discuss the recent developments in expanding the theory to higher dimensions with a focus on the amoeba formalism [36] as well as to the many-body context [18–22]. Moving away from pure theory, we continue by providing a short overview of experimental realizations of the NH skin effect as well as exciting applications of it, namely, the funneling of light [9], the topological Ohmmeter [37, 38], and topological amplification [39, 40]. We end the perspective by discussing what we believe are the open questions in the field.

The NH skin effect: The basics. – We start this perspective with a paradigmatic one-dimensional (1D) example, and discuss several well-known, yet important general properties of the NH skin effect in 1D systems.

The Hatano-Nelson model. The Hatano-Nelson model was first proposed by Hatano and Nelson to study localization transitions in the context of superconductivity [41],
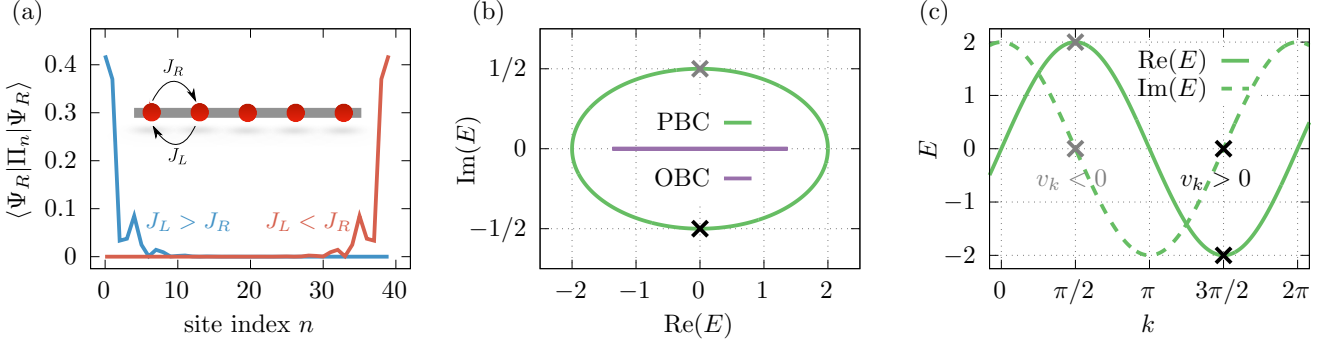
Figure 1: Hatano-Nelson model and its features. (a) Schematic illustration of the model, showing the localization of bulk modes under OBC on the left or right end depending on the relative hopping strengths: For $|J_L| < |J_R|$, modes localize on the right end, while for $|J_L| > |J_R|$, they localize on the left end. (b) Under PBCs, the eigenvalues trace an ellipse in the complex plane, and the eigenstates are extended. In contrast, the OBC spectrum drastically deviates from the PBC spectrum exhibiting purely real eigenvalues and localized eigenmodes manifesting the NH skin effect. (c) The real and imaginary parts of the eigenvalues as a function of k. The gray and black crosses in (b) and (c) indicate the left and right movers in the dispersion, respectively.

and its Hamiltonian, shown in the inset of Fig. 1(a), reads

$$H = \sum_n (J_L c_n^\dagger c_{n+1} + J_R c_{n+1}^\dagger c_n), \qquad (1)$$

with $J_L(J_R) \in \mathbb{R}$ the nearest-neighbor hopping parameter to the left (right), and $c_n^\dagger$ (c_n) creating (annihilating) an excitation on site n. This model is NH when $J_L \neq J_R$. As a 1D single-band model, the energy under PBCs, $E(k)$, corresponds to the Bloch Hamiltonian $H(k)$, and reads $E(k) = (J_L + J_R) \cos k + i(J_L - J_R) \sin k$. As seen in Fig. 1(b), $E(k)$ forms an ellipse and winds around the origin in the complex energy plane as a function of k in the (counter)clockwise direction, when $|J_L| < |J_R|$ ($> |J_R|$). As such, it is possible to define a *spectral* winding number w as [26,27]

$$w = \frac{1}{2\pi i} \int_{-k}^{k} dk \, \partial_k \ln E(k) = \begin{cases} +1, & |J_L| > |J_R|, \\ -1, & |J_L| < |J_R|. \end{cases} \qquad (2)$$

The winding number can only change when $E(k) = 0$ for some k, i.e., when $|J_L| = |J_R|$. Turning to OBCs, it is straightforward to see from the Hamiltonian in Eq. (1), that all eigenstates accumulate on the boundary on the right (left) when $|J_L| < |J_R|$ ($> |J_R|$) as shown in Fig. 1(a). This phenomenon of a piling up of a macroscopic number of states is known as the NH skin effect.

There is an intuitive way to understand the connection between the sign of the spectral winding number and the boundary to which the NH skin states localize. When the winding number is negative (positive), the eigenvalues wind in the (counter)clockwise direction. As the PBC spectrum of the Hatano-Nelson model is centered around zero energy, half of the spectrum is in the positive imaginary plane. That means that for a negative (positive) winding number, the right (left) movers with group velocity $v_k = \text{Re}[\partial_k E(k)] > 0$ (< 0) have positive imaginary energy whereas the left (right) movers have negative imaginary energy, as illustrated in Figs. 1(b,c). In the long-time

limit, the right (left) movers thus dominate the behavior of the system, and one sees that all NH skin states pile up on the right (left) boundary of the system. A similar argument is also presented in Ref. 42.

Localization of skin states. To observe the NH skin effect, one has to study the localization of the right or left eigenstate separately. Indeed, it is shown in Refs. 33,43,44 that if the right eigenstates $|\Psi_R\rangle$, which is obtained by solving $H |\Psi_R\rangle = E |\Psi_R\rangle$, are exponentially localized to one boundary, the left eigenstates $|\Psi_L\rangle$ satisfying $\langle \Psi_L| H = E \langle \Psi_L|$, or alternatively, $H^\dagger |\Psi_L\rangle = E^* |\Psi_L\rangle$, are exponentially localized to the opposite boundary. As a consequence, the *biorthogonal localization* of the right and left eigenstate quantified by $\langle \Psi_L|\Pi_n|\Psi_R\rangle$, where $\Pi_n = c_n^\dagger |0\rangle \langle 0| c_n$ is the projector onto each site n, has weight throughout the system. Thus, the skin states have a bulk-state-like fingerprint in the biorthogonal picture, albeit with potentially negative and/or complex weights.

Generalized Brillouin zone. Next, we note there is an intimate link between the NH skin effect and the so-called generalized Brillouin zone (GBZ). The theory of the GBZ was first developed by Yao and Wang in Ref. 30, and later expanded in Refs. 44,45, in order to restore the breakdown of the conventional bulk-boundary correspondence (cBBC) as observed in models featuring the NH skin effect, which will be discussed in more detail below.

The GBZ $\mathcal{C}$ can be constructed by solving the characteristic equation of the non-Bloch Hamiltonian $H(\beta)$, which is the analytic continuation of the Bloch Hamiltonian. This closed curve $\mathcal{C}$ contains crucial information about the system under OBCs: The OBC spectrum is given by $H(\beta)$ with $\beta \in \mathcal{C}$, and one can determine spatial decay rates for the NH skin modes, which are related to β, in the continuum limit. Indeed, for any skin mode, one finds its associated β, and if $|\beta| < 1$ (> 1), or in other words if $\mathcal{C}$ is inside (outside) of the unit circle [45], the skin state localize to the left (right) boundary. For

$|\beta| = 1$, the state is delocalized as the Bloch states, and the corresponding point is called a Bloch point [45].

Exceptional points. Interestingly, the NH skin effect is accompanied by the appearance of exceptional points (EPs) with an order scaling with system size under OBCs [46, 47]. EPs are degeneracies, which abundantly appear in NH matrices [48, 49], at which not only the eigenvalues but also the eigenvectors coalesce, i.e., the geometric multiplicity is smaller than the algebraic multiplicity [50, 51]. At EPs, the NH matrix features Jordan blocks, whose dimension corresponds to the order of the EP. Close to an EP, eigenvectors start to overlap until they finally coalesce when reaching the EP. We indeed see such a high-order EP for the Hatano-Nelson model, where in the extreme limit $J_R (J_L) = 0$, all states coalesce onto the last left (right) site .

Sensitivity to boundary conditions. As is clearly visible in the spectrum of the Hatano-Nelson model in Fig. 1(b), the spectrum strongly depends on the boundary conditions. In Ref. 52, it is shown that by introducing coupling terms between the ends of 1D chains, one finds that the system crosses several EPs upon tuning tune between OBCs and PBCs [53–55], highlighting a topological distinction between the two cases. Refs. 53, 54 show that the cross-over from OBCs to PBCs, i.e., from having skin states to Bloch states, happens for exponentially small couplings. While it thus may seem that the NH skin effect is not a robust feature, it is shown in Ref. 54 that physically relevant locality constraints exponentially suppress this kind of coupling. Also, further modifications to the boundary conditions result in new localization phenomena and transitions between different behaviors [56].

Beyond Hamiltonians. While usually phrased in terms of Hamiltonians, the skin effect is a property of NH matrices. Thus, any physical system which can be represented by a NH matrix might exhibit the skin effect. Prominent examples include the conductance matrix, which is the appropriate object to consider when handling topoelectric circuits [12], and the damping matrix in open quantum systems [14, 15].

Non-normality and non-reciprocity as requirement of the NH skin effect. – Not all NH matrices feature a NH skin effect, and a necessary criterion needs to be satisfied, namely, the NH matrix needs to be *non-normal* [1], i.e., $[H, H^\dagger] \neq 0$. By writing $H = H_H + iH_A$, with $H_H = H_H^\dagger$ the Hermitian part and $iH_A = -(iH_A)^\dagger$ the anti-Hermitian part of H, non-normality is equivalent to $[H_H, H_A] \neq 0$. If H_H and H_A would commute, H would share an orthogonal eigenbasis with H_H and H_A, which prohibits the existence of skin states.

In Ref. 34, it is shown that non-normality is not a sufficient condition. Additionally, the system needs to be *non-reciprocal*, that is, if its susceptibility matrix, or Green's function, $\chi(\omega) = -i(\omega\mathbb{I} - H)^{-1}$ satisfies $|\chi(\omega)| \neq |\chi(\omega)|^T$, which is equivalent to the scattering matrix S satisfying $|S| \neq |S|^T$, where the modulus of a matrix means the absolute value of each matrix element [57, 58]. Physically, this means that the response of the system is not invariant under exchanging input and output. Importantly, this presented notion of non-reciprocity should not be confused with non-reciprocal hoppings, which in the NH context refers to asymmetric hoppings and in the Hermitian context is sometimes used to indicate the presence of non-zero phases on the hoppings due to pseudo-magnetic fields.

Spectral features, topological protection and the NH bulk-boundary correspondence. – If a NH matrix is both non-normal and non-reciprocal, its PBC spectrum displays a so-called point gap [34]. A point gap is defined as there being a base point E_B, which is not crossed by the complex-energy bands, and crossing this point defines a gap closing transition [27]. Indeed, we see in the example of the Hatano-Nelson model that the PBC spectrum has a point gap, cf. Fig. 1(b), and the gap closes as discussed at $|J_L| = |J_R|$. It has been shown that for the NH skin effect to occur in 1D systems, the PBC spectrum must feature such point gaps [28, 32, 33, 59]. In extension, this means that it is possible to find a non-zero spectral topological invariant for these systems. For example, the spectral winding number in Eq. (2) for arbitrary periodic 1D systems described by the Bloch Hamiltonian $H(k)$, can be generalized to the following form [27]

$$w(E_B) = \frac{1}{2\pi i} \int_{-\pi}^{\pi} dk \, \partial_k \ln\{\det[H(k)] - E_B\}. \quad (3)$$

We note that if one is interested in the state localization of a specific skin state, one has to select its energy as reference energy E_B.

The skin effect as a topological effect is robust against weak perturbations of the system. For example, in the Hatano-Nelson model, cf. Eq. (1), onsite disorder has been studied in Refs. 27, 41, whereas additional perturbations to the hoppings have been addressed in Ref. 60, 61, revealing a stability of the skin states to these disturbances.

These insights regarding the link between a spectral invariant defined under PBCs, and the NH skin effect then leads to the establishment of a *new, truly non-Hermitian bulk-boundary correspondence*: Having point gaps in the PBC spectrum of 1D models quantified by a non-trivial spectral invariant implies the piling up of states on the boundary of the system under OBCs [28, 31–33, 59].

Beyond spectral winding numbers: Symmetries. There are models, which feature a NH skin effect, while having a zero spectral winding number. In these cases, it is possible to find alternative spectral invariants. For example, the presence of so-called time-reversal dagger symmetry (TRS†) [62] with the symmetry operator squaring to minus one results in doubly degenerate loops in the PBC spectrum with opposite winding numbers. As a result half of the skin states accumulate on one boundary and the other half on the other. The spectral invariant is a $\mathbb{Z}_2$ invariant, and this type of skin effect is referred to
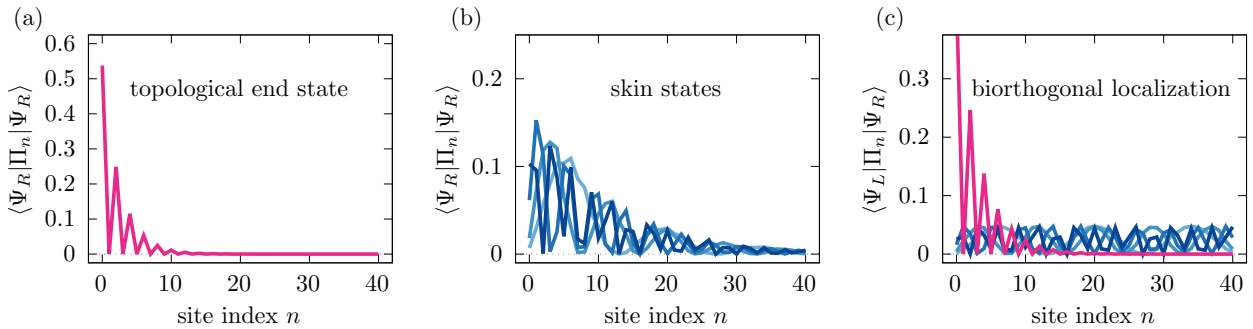
Figure 2: Topological end state and skin state localization. Normalized right wavefunction of (a) topological boundary state in pink and (b) skin states in blues. The end state is localized on a single sublattice whereas the skin modes are distributed across both sublattices. (c) The biorthogonal product of the right and left states shows that the end state remains localized while the skin states are delocalized.

as the $\mathbb{Z}_2$-skin effect [28]. In general, symmetries play an important role in the context of the NH skin effect. Indeed, the presence of certain symmetries prohibits the appearance of the NH skin effect. These symmetries include PT symmetry [47] and pseudo-Hermitian symmetry [62] in the unbroken phase for any-dimensional systems as well as parity symmetry and TRS† with the symmetry operator squaring to one for 1D systems [62].

Topological boundary states and the NH skin states. – Next we turn to the coexistence of skin states and topological boundary states, and discuss how to distinguish them. Previously, we saw that the NH skin effect is protected by spectral topology, specifically the point gap topology unique to NH systems. In contrast, topological boundary states arise from wavefunction topology. If a model features both NH skin states and topological boundary states, it is a priori not obvious, how to distinguish these different types of states. We illustrate a way to make this distinction with an example.

We focus on the anisotropic SSH model described by the Hamiltonian [30, 53]

$$H = \sum_n \left[(t_1 + \gamma)c_{A,n}^\dagger c_{B,n} + (t_1 - \gamma)c_{B,n}^\dagger c_{A,n} \right. \\ \left. + t_2(c_{A,n+1}^\dagger c_{B,n} + c_{B,n+1}^\dagger c_{A,n}) \right], \quad (4)$$

where $c_{\alpha,n}^\dagger$ ($c_{\alpha,n}$) creates (annihilates) a state on sublattice α in unit cell n, t_1 (t_2) is the nearest-neighbor hopping parameters inside (between) unit cells, and γ makes the system NH by changing the magnitude of the hopping to the right with respect to the hopping to the left. This model exhibits sublattice symmetry, which allows for the explicit construction of the topological end states via a destructive interference argument [53]. Such end states are exponentially localized, and only have weight on one of the sublattices, as shown in Fig. 2(a) for a right eigenstate localized to the left boundary. Due to the anisotropy factor γ, all the other states pile up on one of the boundaries, cf. Fig. 2(b), thus displaying the NH skin effect. Let us now answer the questions as to how to distinguish the

topological boundary states from the skin states.

The answer to this question lies in the *biorthogonal properties* of these states. While the skin states behave as bulk states when studying their biorthogonal localization, as we already discussed for the Hatano-Nelson model, topological boundary states will remain localized to the boundary, as shown in Fig. 2(c). We note that situations may also arise in which the right eigenstate of a boundary state solution is localized to the opposite boundary as compared to the left eigenstate, as also mentioned in Ref. 37 in the context of topological sensors discussed below. In this case, the biorthogonal product of the right and left topological boundary state will still show a stronger signature to one of the boundaries, while preserving its general profile.

As an interesting side note, we remark that this model breaks the cBBC [30,53], where a topological invariant defined from the Bloch Hamiltonian predicts the existence of modes on the boundaries. The previously mentioned GBZ approach provides a route towards restoring the cBBC [30,44,45], whereas an alternative approach based on the biorthogonal properties of the boundary modes was proposed in Ref. 53. This breakdown of the cBBC first noticed in Ref. 63 is a common feature of "conventional" topological models featuring the NH skin effect [47], and can be intuitively understood from the fact due a discrepancy between the PBC and OBC spectra, gap closings indicating topological phase transitions generally occur for different parameter values.

Skin effect in higher dimensions. – So far we have only considered the appearance of skin states in 1D systems. In higher dimension, there is not yet an all-encompassing theory. Efforts in this direction have been made very recently with the development of the *amoeba formalism* [36]. The amoeba, which is a mathematical region in $\mathbb{R}^d$ having holes and narrowing tentacles extending to infinity, is a very recent addition to algebraic geometry resembling its biological prototype [64]. In particular, the formalism relies on the principle that all algebraic-geometric information has to be encoded in the charac-

teristic polynomials of the NH model described by the Bloch Hamiltonian. The amoeba formulation, combined with its dual Newton polygon formalism [65] and tropical geometric framework [66], provides a unified approach to characterize the NH skin effect [36, 67–70].

Let us discuss this with a simple example of a single-band model in two dimensions (2D) [36], shown in Fig. 3(a). Its Hamiltonian reads

$$H = \sum_{n,m} \Big[J_L \left(c_{n,m}^\dagger c_{n+1,m} + c_{n,m+1}^\dagger c_{n,m} \right) \tag{5}$$
$$+ J_R \left(c_{n+1,m}^\dagger c_{n,m} + c_{n,m}^\dagger c_{n,m+1} \right)$$
$$+ t' \left(c_{n,m}^\dagger c_{n+1,m+1} + c_{n,m+1}^\dagger c_{n+1,m} + H.c. \right) \Big],$$

where $c_{n,m}^\dagger$ ($c_{n,m}$) creates (annihilates) an excitation on site (n,m) in the 2D lattice, and J_L and J_R (t') are the (next-)nearest neighbor hoppings. To determine the Bloch Hamiltonian, one Fourier transforms to introduce the two Bloch momenta k_x and k_y. Likewise to the GBZ theory, one analytically continues $k_{x,y}$, and replaces the plane waves (e^{ik_x}, e^{ik_y}) by the complex functions (β_y, β_y) to find the non-Bloch Hamiltonian $H(\beta_x, \beta_y)$. Then, the key lies in the solution of its characteristic equation

$$\det[E - H(\beta_x, \beta_y)] = 0. \tag{6}$$

Without solving this polynomial fully for β_x and β_y, one can express $\beta_y(E)$ as function of $\beta_x(E)$ as $\beta_{y,a}(\beta_x, E)$, where a labels the different solutions in β_x, in our example $a = 1, 2$. Then, by plotting $\log |\beta_x(E)|$ against $\log |\beta_{y,a}(E)|$ for any a and E we get an amoeba, depicted in Fig. 3(b). If *any* amoeba for *any* a contains *no* central hole, E belongs to the OBC spectrum, and one can construct the full OBC spectrum in this fashion. The associated Ronkin function then provides insight into the skin state localization lengths [36]. In 1D, the construction of the amoeba reduces to the construction of the GBZ.

As a side note, we remark that the NH skin effect may also appear on higher-order boundaries in higher-dimensional models [29,71–73], and has also been observed in higher-dimensional non-periodic systems such as quasicrystals and amorphous networks as well as fractals lattices [74].

Skin effect in many-body systems. – Next, we discuss the NH skin effect in the many-body context, which is an active topic of current research with significant differences between fermionic and bosonic systems. The many-body scenario is more intricate in the fermionic case due to the interplay of non-orthogonal eigenstructures and Pauli's exclusion principle [20]. Furthermore, the fermionic repulsion significantly alters the occupied orbitals, ensuring that no more than one fermion, or one hard-core boson, can occupy each physical site. Consequently, the exponential localization of all fermions at a boundary is impossible [18,19]. In Ref. 20, it is shown that
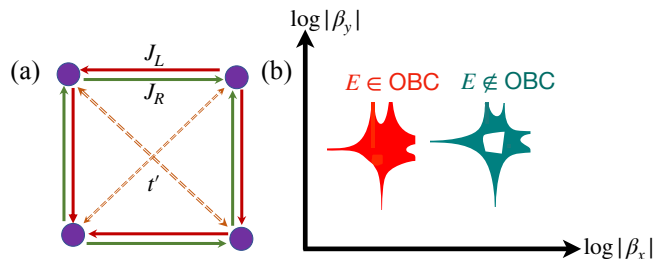

Figure 3: Amoeba formulation in 2D. (a) Illustration of the 2D single-band model with asymmetric hopping in Eq. (5). (b) The plots depict 2D amoeba, where the points $(\log |\beta_x|, \log |\beta_y|)$ satisfy the characteristic equation in Eq. (6). A hole appears in the amoeba for energies outside the OBC spectrum, while no hole is present for energies within the OBC spectrum. The disappearance of the hole in the amoeba provides crucial information about the GBZ in the 2D system.

the many-body skin effect results from an imbalance in the density distribution rather than just a sum of exponential orbitals due to the exclusion principle. The degree of asymmetry in this distribution quantifies the exponential localization of the skin modes as the system size increases. In Ref. 22, a general criterion for the appearance of the NH skin effect in many-body systems, known as the Fock-space skin effect, is discussed. Beyond the Pauli principle, interactions enrich the phenomenology of the skin effect. For instance, attractive interactions may cause clustering and thus localization, while repulsive interactions promote delocalization. In contrast to fermionic models, nonreciprocal bosonic models with interacting bosons lead to particle accumulation at the edges, forming a skin superfluid state along with distinct Mott-insulating regimes [75]. Ref. 21 introduces the NH Mott skin effect in a bosonic chain with spin degrees of freedom, emphasizing the interaction between strong correlations and NH point-gap topology.

Turning to the properties of these systems, it has been shown that the skin effect suppresses entanglement propagation hindering thermalization [76]. This leads to an area law for the entanglement entropy of the non-equilibrium steady state [77], in contrast to a volume law in Hermitian systems. Many more interesting effects are predicted in the many-body context, such as skin clustering leading to Hilbert space fragmentation [78], many-body localization [79], multifractality [80], and multipole skin effect [81].

Experimental realizations and applications. – The non-Hermitian skin effect has been observed in a plethora of classical experimental platforms, such as in coupled fiber loops [9], mechanical metamaterials [11], topoelectric circuits [12], quantum walks [10], acoustic metamaterials [13], and nano-optomechanical networks [40]. Signatures of the skin effect have also been seen in a few quantum setups such as in cold atoms [23] and in a multi-termal quantum Hall device [82]. While the skin effect can only be observed by measuring the right or left

eigenstates separately, there are observables that crucially depend on the interplay between both. Schomerus shows in the context of non-reciprocal metamaterials that while the dynamical response of such systems gives direct information on the right and left eigenvectors separately, the overall sensitivity is governed by the biorthogonal properties of these eigenmodes [83].

Beyond observing the existence of skin states, some studies focus on harnessing this effect for real world applications. For example, the aforementioned experiment in fiber loops proposes a topological funnel for light [9]. In this setup, two anisotropic 1D chains with opposite winding numbers are coupled to each other so that the skin effect in both chains conspires to act as a funnel resulting in an accumulation of all excitations at the interface. Another proposal to employ the NH skin effect is in the context of NH topological sensors [37]. Here it is shown that coupling the ends of the anisotropic SSH model, cf. Eq. (4), results in an exponential splitting of the eigenvalues, such that perturbing this coupling leads to an exponentially strong response. A crucial ingredient in this context is the presence of a single topological end state, whose right and left eigenvectors localize on opposite ends. This mechanism is exploited in the experimental realization of the NH topological ohmmeter in Ref. 38. The skin effect has also been related to directional amplification in driven-dissipative cavity arrays [34,39]. Here, a signal entering a NH chain, similar to the Hatano-Nelson model in Eq. (1), at one end gets exponential amplified towards the other end, while it gets exponential suppressed in the other direction. This principle has been experimentally verified in a nano-optomechanical network in Ref. 40.

Summary and Outlook. – In summary, we systematically explored the underlying mechanisms driving the NH skin effect demonstrating how it fundamentally shapes NH phases. We started by discussing several well-known features of the NH skin effect before shifting our focus to what we believe are some of the most interesting properties associated with it. After discussing how non-normality and non-reciprocity are necessary ingredients to generate a NH skin effect in NH systems, we continued by exploring the general properties of the NH skin effect, including its spectral characteristics and topological protection. Additionally, we reviewed how skin modes can be distinguished from topological boundary modes by analyzing their biorthogonal footprint. The NH skin effect in higher dimensions was discussed focusing on the recent amoeba formalism. Lastly, we explored the NH skin effect in many-body scenarios, and surveyed the experimental advances and applications.

We end this perspective with an outlook. While the NH skin effect and non-Bloch theory are well understood in 1D systems, a rigorous theoretical framework is needed for higher dimensions. Exploring connections to modern mathematics [36, 68], including K-theory and symmetry classifications, offers promising avenues for uncovering and

engineering NH skin effects in higher-dimensional systems. At the same time, the interplay between interactions in NH topological phases and skin modes still needs to be fully understood. Recent simulations on skin clustering in strongly interacting bosonic systems, highlighting the fragmented Hilbert space [84], reveal new connections to phenomena like the eigenstate thermalization hypothesis and quantum scars. Extensions of the NH skin effect in 2D correlated fermion systems open new avenues for exploring many-body skin effects in higher dimensions [85]. Additionally, the impact of time-periodic driving on NH skin effects in single-particle and interacting many-body systems presents a fascinating frontier for future research [86, 87]. Another important aspect is to understand the time dynamics and steady state nature of such NH skin modes in open quantum systems [14]. Also, we want to highlight that the introduction of nonlinearities enrich the phenomenology of the skin effect [88], leading to modified localization properties, such as trap-skin states [89], and in general phenomena beyond established topological theories [90,91].

$* * *$

References

[1] BERGHOLTZ E. J., BUDICH J. C. and KUNST F. K., *Reviews of Modern Physics*, **93** (2021) 015005.

[2] YUTO ASHIDA Z. G. and UEDA M., *Advances in Physics*, **69** (2020) 249.

[3] OKUMA N. and SATO M., *Annual Review of Condensed Matter Physics*, **14** (2023) 83.

[4] BENDER C. M. and BOETTCHER S., *Phys. Rev. Lett.*, **80** (1998) 5243.

[5] BENDER C. M., *Reports on Progress in Physics*, **70** (2007) 947.

[6] EL-GANAINY R., MAKRIS K. G., KHAJAVIKHAN M., MUSSLIMANI Z. H., ROTTER S. and CHRISTODOULIDES D. N., *Nature Physics*, **14** (2018) 11.

[7] MIRI M.-A. and ALÙ A., *Science*, **363** (2019) eaar7709.

[8] ÖZDEMIR Ş. K., ROTTER S., NORI F. and YANG L., *Nature Materials*, **18** (2019) 783.

[9] WEIDEMANN S., KREMER M., HELBIG T., HOFMANN T., STEGMAIER A., GREITER M., THOMALE R. and SZAMEIT A., *Science*, **368** (2020) 311.

[10] XIAO L., DENG T., WANG K., ZHU G., WANG Z., YI W. and XUE P., *Nature Physics*, **16** (2020) 761.

[11] GHATAK A., BRANDENBOURGER M., VAN WEZEL J. and COULAIS C., *Proceedings of the National Academy of Sciences*, **117** (2020) 29561.

[12] HELBIG T., HOFMANN T., IMHOF S., ABDELGHANY M., KIESSLING T., MOLENKAMP L. W., LEE C. H., SZAMEIT A., GREITER M. and THOMALE R., *Nature Physics*, **16** (2020) 747.

[13] ZHANG L., YANG Y., GE Y., GUAN Y.-J., CHEN Q., YAN Q., CHEN F., XI R., LI Y., JIA D., YUAN S.-Q., SUN H.-X., CHEN H. and ZHANG B., *Nature Communications*, **12** (2021) 6297.

[14] SONG F., YAO S. and WANG Z., *Phys. Rev. Lett.*, **123** (2019) 170401.

[15] YANG F., JIANG Q.-D. and BERGHOLTZ E. J., *Phys. Rev. Res.*, **4** (2022) 023160.

[16] NAKAMURA Y. and HATANO N., *Physica B: Condensed Matter*, **378-380** (2006) 292.

[17] NAKAGAWA M., TSUJI N., KAWAKAMI N. and UEDA M., *Phys. Rev. Lett.*, **124** (2020) 147203.

[18] LEE E., LEE H. and YANG B.-J., *Physical Review B*, **101** (2020) 121109.

[19] LIU T., HE J. J., YOSHIDA T., XIANG Z.-L. and NORI F., *Physical Review B*, **102** (2020) 235151.

[20] ALSALLOM F., HERVIOU L., YAZYEV O. V. and BRZEZIŃSKA M., *Physical Review Research*, **4** (2022) 033122.

[21] YOSHIDA T., ZHANG S.-B., NEUPERT T. and KAWAKAMI N., *Physical Review Letters*, **133** (2024) 076502.

[22] SHIMOMURA K. and SATO M., *Physical Review Letters*, **133** (2024) 136502.

[23] LIANG Q., XIE D., DONG Z., LI H., LI H., GADWAY B., YI W. and YAN B., *Physical review letters*, **129** (2022) 070401.

[24] NELSON D. R. and SHNERB N. M., *Phys. Rev. E*, **58** (1998) 1383.

[25] LUBENSKY D. K. and NELSON D. R., *Phys. Rev. Lett.*, **85** (2000) 1572.

[26] SHEN H., ZHEN B. and FU L., *Phys. Rev. Lett.*, **120** (2018) 146402.

[27] GONG Z., ASHIDA Y., KAWABATA K., TAKASAN K., HIGASHIKAWA S. and UEDA M., *Physical Review X*, **8** (2018) 031079.

[28] OKUMA N., KAWABATA K., SHIOZAKI K. and SATO M., *Physical Review Letters*, **124** (2020) 086801.

[29] ZHANG K., YANG Z. and FANG C., *Nature Communications*, **13** (2022) 2496.

[30] YAO S. and WANG Z., *Physical Review Letters*, **121** (2018) 086803.

[31] BORGNIA D. S., KRUCHKOV A. J. and SLAGER R.-J., *Physical Review Letters*, **124** (2020) 056802.

[32] ZHANG K., YANG Z. and FANG C., *Physical Review Letters*, **125** (2020) 126402.

[33] KOEKENBIER L. and SCHULZ-BALDES H., *J. Spectr. Theory*, (2024).

[34] BRUNELLI M., WANJURA C. C. and NUNNENKAMP A., *SciPost Phys.*, **15** (2023) 173.

[35] BRODY D. C., *J. Phys. A: Math. Theor.*, **47** (2013) 35305.

[36] WANG H.-Y., SONG F. and WANG Z., *Physical Review X*, **14** (2024) 021011.

[37] BUDICH J. C. and BERGHOLTZ E. J., *Phys. Rev. Lett.*, **125** (2020) 180403.

[38] KÖNYE V., OCHKAN K., CHYZHYKOVA A., BUDICH J. C., VAN DEN BRINK J., FULGA I. C. and DUFOULEUR J., *Phys. Rev. Appl.*, **22** (2024) L031001.

[39] WANJURA C. C., BRUNELLI M. and NUNNENKAMP A., *Nature Communications*, **11** (2020) 3149.

[40] SLIM J. J., WANJURA C. C., BRUNELLI M., DEL PINO J., NUNNENKAMP A. and VERHAGEN E., *Nature*, **627** (2024) 767.

[41] HATANO N. and NELSON D. R., *Physical Review Letters*, **77** (1996) 570.

[42] LEE J. Y., AHN J., ZHOU H. and VISHWANATH A., *Phys. Rev. Lett.*, **123** (2019) 206404.

[43] BÖTTCHER A. and GRUDSKY S., *Spectral properties of banded Toeplitz matrices* (SIAM) 2005.

[44] YOKOMIZO K. and MURAKAMI S., *Phys. Rev. Lett.*, **123** (2019) 066404.

[45] SONG F., YAO S. and WANG Z., *Physical Review Letters*, **123** (2019) 246801.

[46] MARTINEZ ALVAREZ V. M., BARRIOS VARGAS J. E. and FOA TORRES L. E. F., *Physical Review B*, **97** (2018) 121401.

[47] KUNST F. K. and DWIVEDI V., *Physical Review B*, **99** (2019) 245116.

[48] BERRY M., *Czechoslovak Journal of Physics*, **54** (2004) 1039.

[49] BUDICH J. C., CARLSTRÖM J., KUNST F. K. and BERGHOLTZ E. J., *Phys. Rev. B*, **99** (2019) 041406.

[50] KATO T., *Perturbation theory of linear operators* (Springer, Berlin) 1966.

[51] HEISS W. D., *Journal of Physics A: Mathematical and Theoretical*, **45** (2012) 444016.

[52] XIONG Y., *Journal of Physics Communications*, **2** (2018) 035043.

[53] KUNST F. K., EDVARDSSON E., BUDICH J. C. and BERGHOLTZ E. J., *Physical Review Letters*, **121** (2018) 026808.

[54] KOCH R. and BUDICH J. C., *The European Physical Journal D*, **74** (2020) 70.

[55] ROCCATI F., *Physical Review A*, **104** (2021) 022215.

[56] LI L., LEE C. H. and GONG J., *Communications Physics*, **4** (2021) 42.

[57] JALAS D., PETROV A., EICH M., FREUDE W., FAN S., YU Z., BAETS R., POPOVIĆ M., MELLONI A., JOANNOPOULOS J. D., VANWOLLEGHEM M., DOERR C. R. and RENNER H., *Nature Photonics*, **7** (2013) 579.

[58] CALOZ C., ALÙ A., TRETYAKOV S., SOUNAS D., ACHOURI K. and DECK-LÉGER Z.-L., *Phys. Rev. Appl.*, **10** (2018) 047001.

[59] NAKAMURA D., BESSHO T. and SATO M., *Physical Review Letters*, **132** (2024) 136401.

[60] CLAES J. and HUGHES T. L., *Physical Review B*, **103** (2021) L140201.

[61] WANJURA C. C., BRUNELLI M. and NUNNENKAMP A., *Physical Review Letters*, **127** (2021) 213601.

[62] KAWABATA K., SHIOZAKI K., UEDA M. and SATO M., *Phys. Rev. X*, **9** (2019) 041015.

[63] LEE T. E., *Phys. Rev. Lett.*, **116** (2016) 133903.

[64] GELFAND I. M., KAPRANOV M. M. and ZELEVINSKY A. V., *A-discriminants* in *Discriminants, Resultants, and Multidimensional Determinants* (Springer) 1994 pp. 271–296.

[65] BRIESKORN E. and KNÖRRER H., *Plane Algebraic Curves: Translated by John Stillwell* (Springer Science & Business Media) 2012.

[66] MACLAGAN D. and STURMFELS B., *Graduate Studies in Mathematics*, **161** (2009) 75.

[67] JAISWAL R., BANERJEE A. and NARAYAN A., *New Journal of Physics*, **25** (2023) 033014.

[68] BANERJEE A., JAISWAL R., MANJUNATH M. and NARAYAN A., *Proceedings of the National Academy of Sciences*, **120** (2023) e2302572120.

[69] WANG S.-X., *Physical Review B*, **109** (2024) L081108.

[70] HU H., *Science Bulletin*, (2024) .

[71] LEE C. H., LI L. and GONG J., *Phys. Rev. Lett.*, **123** (2019) 016805.

[72] EDVARDSSON E., KUNST F. K. and BERGHOLTZ E. J., *Phys. Rev. B*, **99** (2019) 081302.

[73] KAWABATA K., SATO M. and SHIOZAKI K., *Phys. Rev. B*, **102** (2020) 205118.

[74] MANNA S. and ROY B., *Communications Physics*, **6** (2023) 10.

[75] ZHANG D.-W., CHEN Y.-L., ZHANG G.-Q., LANG L.-J., LI Z. and ZHU S.-L., *Physical Review B*, **101** (2020) 235150.

[76] ABANIN D. A., ALTMAN E., BLOCH I. and SERBYN M., *Reviews of Modern Physics*, **91** (2019) 021001.

[77] KAWABATA K., NUMASAWA T. and RYU S., *Physical Review X*, **13** (2023) 021007.

[78] SHEN R. and LEE C. H., *Communications Physics*, **5** (2022) 238.

[79] WANG Y.-C., SUTHAR K., JEN H., HSU Y.-T. and YOU J.-S., *Physical Review B*, **107** (2023) L220205.

[80] HAMANAKA S. and KAWABATA K., *arXiv preprint arXiv:2401.08304*, (2024) .

[81] GLIOZZI J., DE TOMASI G. and HUGHES T. L., *Physical Review Letters*, **133** (2024) 136503.

[82] OCHKAN K., CHATURVEDI R., KÖNYE V., VEYRAT L., GIRAUD R., MAILLY D., CAVANNA A., GENNSER U., HANKIEWICZ E. M., BÜCHNER B., VAN DEN BRINK J., DUFOULEUR J. and FULGA I. C., *Nature Physics*, **20** (2024) 395.

[83] SCHOMERUS H., *Physical Review Research*, **2** (2020) 013058.

[84] ZHANG W., DI F., YUAN H., WANG H., ZHENG X., HE L., SUN H. and ZHANG X., *Physical Review B*, **105** (2022) 195131.

[85] YOSHIDA T., *Physical Review B*, **103** (2021) 125145.

[86] ZHOU L. and ZHANG D.-J., *Entropy*, **25** (2023) .

[87] FAUGNO W. N. and OZAWA T., *Phys. Rev. Lett.*, **129** (2022) 180401.

[88] YUCE C., *Physics Letters A*, **408** (2021) 127484.

[89] EZAWA M., *Physical Review B*, **105** (2022) 125421.

[90] YOSHIDA T., ISOBE T. and HATSUGAI Y., *arXiv preprint arXiv:2407.20895*, (2024) .

[91] WANG S., WANG B., LIU C., QIN C., ZHAO L., LIU W., LONGHI S. and LU P., *arXiv preprint arXiv:2409.19693*, (2024) .